



Assessment of the risks of N-loss to groundwater from data on N-balance surplus in Spanish crops: An empirical basis to identify Nitrate Vulnerable Zones

Mercedes Arauzo ^{a,*}, Gema García ^a, María Valladolid ^b

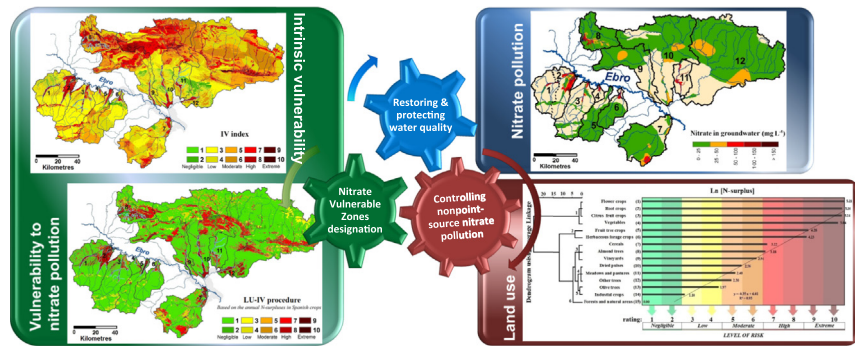
^a Instituto de Ciencias Agrarias, Consejo Superior de Investigaciones Científicas (CSIC), Serrano 115 dpdo., 28006 Madrid, Spain

^b Museo Nacional de Ciencias Naturales, Consejo Superior de Investigaciones Científicas (CSIC), José Gutiérrez Abascal 2, 28006 Madrid, Spain

HIGHLIGHTS

- Most of the alluvial aquifers showed nitrate concentrations above 50 mg L⁻¹.
- Catchment size was revealed as a key factor in the emergence of polluted areas.
- N-surpluses in Spanish crops were used to establish ratings of the risks of N-loss.
- Models using empirical ratings were the best predictors of nitrate pollution.
- Results confirmed the high level of reliability of the LU-IV procedure.

GRAPHICAL ABSTRACT



ARTICLE INFO

Article history:

Received 25 March 2019

Received in revised form 31 July 2019

Accepted 31 July 2019

Available online xxx

Editor: José Virgilio Cruz

Keywords:

Alluvial aquifer

Catchment area

Groundwater vulnerability

LU-IV procedure

Mediterranean area

ABSTRACT

The aim of this research was to conduct an empirical assessment of the risks of N-loss to groundwater associated with land use (LU), based on annual data on the net N-balance surplus in Spanish crops. These data were used to generate a detailed risk rating system reflecting the potential risks of N-loss from agriculture. The new LU ratings were used to assess the specific vulnerability of groundwater to nitrate pollution, by using the LU-IV procedure (Arauzo 2017).

The study area included the catchment areas of 12 alluvial aquifers associated to tributaries of the Ebro River (Spain). Most of the alluvial aquifers were chronically polluted by nitrate, with only a few remaining unaffected by pollution. The LU maps from two different base maps (MCAE 2000–09; SIOSE 2011) were used to generate the respective versions of the map of vulnerability to nitrate pollution using the LU-IV procedure. Potential nitrate vulnerable zones (NVZ) were extracted from different models of vulnerability for comparison with the map of groundwater nitrate content. The models compared were the following: model A (LU-IV procedure, based on MCAE 2000–09 and using LU ratings from N-surpluses in Spanish crops), model B (LU-IV procedure, based on SIOSE 2011 and using LU ratings from N-surpluses in Spanish crops), model C (LU-IV procedure, based on MCAE 2000–09 and using LU ratings from bibliographical references; Arauzo, 2017), model D (IV index), model E (DRASTIC index), and model F (GOD index).

* Corresponding author at: Dpto. de Suelo, Planta y Calidad Ambiental, Instituto de Ciencias Agrarias (ICA), Consejo Superior de Investigaciones Científicas (CSIC), Serrano 115 dpdo., 28006 Madrid, Spain.

E-mail address: mercedes.arauzo@csic.es (M. Arauzo).

Results confirmed, as expected, that models A and B proved to be the best risk predictors, both for polluted groundwater areas and for areas at risk of being polluted. These results support the high level of reliability of the LU–IV procedure, when applying the *LU* ratings obtained empirically from the N-surpluses.

© 2019 Elsevier B.V. All rights reserved.

1. Introduction

More efficient use and management of water are critical to addressing the growing demand for water, threats to water security and the increasing severity of droughts and floods resulting from climate change (goal 6 of the 2030 Agenda for Sustainable Development, to ensure availability and sustainable management of water and sanitation for all; [Economic and Social Council of the United Nations, 2018](#)).

Water pollution by nitrates is one of the environmental challenges facing the international community. The globalisation of water pollution by nitrates is a clear example of the difficulties in addressing nonpoint source pollution throughout the planet. Nitrate concentrations are often high enough to affect water quality, posing a risk to human health and contributing to eutrophication of aquatic ecosystems ([European Environment Agency, 2017](#); [Sutton et al., 2011](#)).

In the European Union (EU), the Nitrates Directive (91/676/EEC; [Council of the European Communities, 1991](#)) establishes that water resources should be considered affected by nitrate pollution when nitrate concentration exceeds 50 mg L^{-1} . The Directive requires areas of land that drain into waters polluted by nitrates to be designated as Nitrate Vulnerable Zones (NVZ). Designations must be reviewed every four years. Farmers having crops in NVZ have to follow mandatory measures within action programmes, limiting N-fertilization and animal manure application to prevent nitrate leaching and runoff.

One of the difficulties faced in the implementation of the EU environmental policies for nitrate pollution control is the lack of a consensus on the criteria for designating NVZ ([De Clercq et al., 2001](#); [Pisciotta et al., 2015](#)), which in turn may limit the success of action programmes in poorly defined vulnerable areas ([Arauzo, 2017](#); [Arauzo and Martínez-Bastida, 2015](#); [Worrall et al., 2009](#)). In this regard, it is clear that additional work is required to improve accuracy in NVZ designations and the efficiency of action programmes ([Commission of the European Communities, 2007](#); [Arqued, 2018](#)).

[Kumar et al. \(2015\)](#) reported that groundwater vulnerability maps have been useful tools to assist government bodies in establishing policies related to the planning of land use and water resource management over the last few decades, with index-based groundwater vulnerability mapping models the most widespread. These authors recognised, however, the existence of research gaps related to risk mapping, assessment techniques and scientific considerations behind the inclusion/exclusion of parameters and the relative ratings and weights assigned to them. [Machiwal et al. \(2018\)](#) likewise pointed out the urgent need for developing a scientifically robust and versatile methodology for the evaluation of intrinsic and specific groundwater vulnerability under varying hydrogeologic and hydro-climatic conditions, suggesting that more studies should be devoted to vulnerability assessment using a 'source-pathway-receptor' approach at basin scale.

The LU–IV procedure ([Arauzo, 2017](#)) was recently developed and validated in an attempt to address the above-stated challenges. It was proposed to assess, in a relative simple way, the specific groundwater vulnerability to nitrate pollution and, in turn, delineate with more precision the NVZ. The procedure combines a map of groundwater intrinsic vulnerability (based on the IV index; [Arauzo, 2017](#)) and a map of the risks of N-loss to groundwater associated with land use (*LU* map) by applying the logical tools of a geographic information system (GIS). Its use facilitates the updating of map-specific vulnerability, when land uses change and maps become obsolete (which could be of interest for periodical revisions of the designated NVZ). When compared with other widely used parametric models of vulnerability (such as DRASTIC

model, by [Aller et al., 1987](#), and GOD model, by [Foster, 1987](#)), the LU–IV procedure proved to be the most effective for assessing vulnerability to nitrate pollution.

This research specifically focuses on the role of land use as a key parameter for a more holistic approach to assessing the vulnerability of groundwater to nitrate pollution by using the LU–IV procedure. To generate an accurate *LU* map, the first requirement is a land use base map (preferably at a scale of at least 1:50,000) and, second, a fine-tuned risk rating system that represents the risks associated with the different land uses (*LU* ratings assigned to the base map). There is, however, still a lack of a reliable set of empirical ratings of the risks of N-loss to groundwater associated with human activities, particularly with regard to non-point agricultural sources (since nitrogen fertilization represents the most important input of nitrate into groundwater; [Sutton et al., 2011](#)). In the absence of an empirical rating system, some authors ([Arauzo, 2017](#); [Martínez-Bastida et al., 2010](#)) extracted the *LU* ratings from bibliographical sources ([Secunda et al., 1998](#)), which could have led to the introduction of some inaccuracies in the models of specific vulnerability to nitrate pollution.

In view of the available data on N-losses to the EU environment, the [European Environment Agency \(2017\)](#) has recently warned that the EU maintains an unacceptable surplus of nitrogen in agricultural land. For that reason, the identification and analysis of the risks of N-losses from agriculture could provide an empirical support for better assessing the vulnerability of groundwater to nitrate pollution.

An environmental indicator of nitrogen pressure from agricultural sources is the Gross Nitrogen Balance (gross N-balance), which represents the difference between nitrogen inputs and nitrogen outputs per unit area of cultivated land ([European Commission, 2018](#)). A positive balance (surplus) reflects inputs that are in excess of crop needs, which can result in diffuse pollution of water (mainly as nitrates) and air (as ammonia and other greenhouse gases). The net N-balance is the gross N-balance minus total nitrogen emissions.

Since net N-balance surpluses tend to leave the system *via* leaching, we set out to use N-surplus data as predictive indicators of the potential impacts of agricultural crops on groundwater quality. So, our first objective was to conduct an assessment of the risks of N-loss to groundwater associated with land use, based on annual data on the net N-balance surplus in Spanish crops from 2011 to 2015 ([MAGRAMA, 2013, 2015a](#); [MAPAMA, 2016, 2017](#)). The annual N-surpluses were used to fine-tune the ratings of the risks associated with the different land use classes and crop types at national scale.

The second objective was to test the new ratings (obtained from the N-surpluses in Spanish crops) which, in turn, were applied to a land use map to generate an optimised version of the *LU* map. For this, initially, two different maps of land use in Spain ([MARM, 2009](#); [SIOSE, 2011](#)) were tested for use as the base map to generate the *LU* map. Both new versions of the *LU* map were used to generate maps of vulnerability to nitrate pollution, according to the LU–IV procedure. Other maps of groundwater vulnerability, based on previous models for assessing groundwater vulnerability (DRASTIC, GOD and the first version of the LU–IV procure, 2017), were also generated, and then tested and compared with the maps resulting from the LU–IV procedure using the new ratings of the risks associated with land use. The thematic maps of all the tested models covered a territory that included the catchment areas of 12 alluvial aquifers associated to tributaries of the Ebro River basin (Spain). Some of these aquifers were chronically affected by nitrate pollution, while others remained practically unaffected. The diversity of environments offered an interesting scenario to analyse specific

aspects of groundwater vulnerability to nitrate pollution linked to land uses. Variability between catchments provided the necessary conditions to explore and validate the best models for vulnerability using statistical approaches.

2. Study area

The assessment of the risks of N-loss to groundwater from agricultural sources (based on the N-surpluses; 1st objective) was conducted on a national scale. A Mediterranean type agriculture dominates in the east and south of Spain, distinguished by erratic rainfall, mild temperatures and a predominance of orchard farming, vegetable and cereal cultivation, olive groves and vineyards. Extensive agriculture (mainly cereals) is predominant in the rest of the territory, with continental-Mediterranean and Atlantic climate influences. Intensive farming is widely practised in most of the alluvial valleys throughout the country (MARM, 2009).

A study area of smaller extension was selected to test the new ratings from the N-surpluses and applied to the LU-IV procedure (2nd objective). The territory encompassed the catchment areas of 12 alluvial aquifers associated to tributaries of the Ebro River basin (Spain; Fig. 1 and Table 1). The catchments covered a total area of 16,408 km². Different types of aquifer occupied 10,484 km², of which 734 km² corresponded to 12 alluvial groundwater bodies (Table 1) and the rest to 18 non-alluvial groundwater bodies (mainly carbonate aquifers, but also detrital sedimentary aquifers). The climate is continental-Mediterranean, although a mountain climate prevails in the mountainous areas (Pyrenees, Basque mountains and Iberian System; Fig. 1). Annual rainfall ranged from 360 to 1527 mm (Table 1), varying according

to altitude. The territory supports a variety of land uses, some of which are major anthropogenic sources of N-input mostly related to agricultural activities (MARM, 2009).

The 12 alluvial aquifers present different levels of nitrate pollution as a result of the characteristics of their catchments (hydrology, lithology, topography, climate and land use).

Most of the non-alluvial groundwater bodies belong to interbasin systems (Fig. 1) which are transversally situated in the upper-middle section of the alluvial basins. Although these groundwater bodies are practically unaffected by nitrate pollution, they were included in the research since they play a key role in the hydrological dynamics of the alluvial catchments. More detailed information on these non-alluvial groundwater bodies can be found in Arauzo (2017).

To date, only five of the 12 catchments under study have areas officially designated as NVZ by the Spanish Government (Confederación Hidrográfica del Ebro, 2018; Table 1), jointly covering a surface of 354 km².

3. Material and methods

3.1. Risk assessment of N-losses associated with land use

The gross N-balance depicts the difference between N-inputs (from mineral fertilisers, manure, other organic fertilisers, seed and planting materials, biological N fixation by leguminous crops and free living organisms, and atmospheric N deposition) and N-outputs (removal of nitrogen with the harvest of crops and grazing of fodder, crop residuals removed from the field) per hectare of utilised agricultural land. The net N-balance is the gross N-balance minus total nitrogen emissions

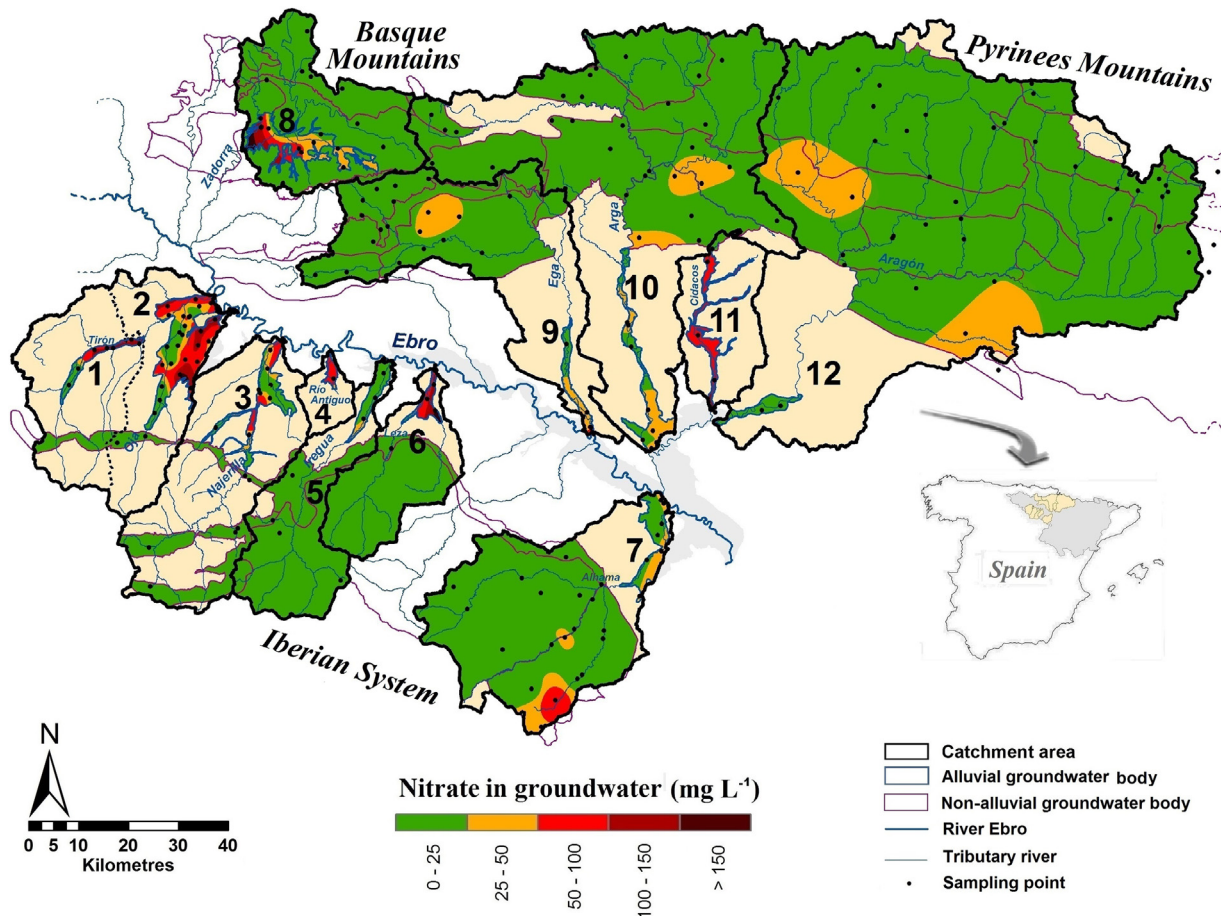


Fig. 1. Study area: catchment areas of 12 alluvial aquifers associated to tributaries of the Ebro River basin (Spain); the spatial distribution of nitrate content in groundwater, based on mean concentrations from 2011 to 2015 at 290 monitoring points, is also shown; the 12 catchment areas are numbered as in Table 1.

Table 1
Catchment characteristics of the 12 alluvial aquifers.

Name and code number:	Tirón Alluvial Aquifer catchment (1)	Oja Alluvial Aquifer catchment (2)	Najerilla Alluvial Aquifer catchment (3)	Río Antiguo Alluvial Aquifer catchment (4)	Iregua Alluvial Aquifer catchment (5)	Leza Alluvial Aquifer catchment (6)	Alhama Alluvial Aquifer catchment (7)	Vitoria Alluvial Aquifer catchment (8)	Ega Alluvial Aquifer catchment (9)	Arga Alluvial Aquifer catchment (10)	Cidacos Alluvial Aquifer catchment (11)	Alto Aragón Alluvial Aquifer catchment (12)
Total catchment area (TCA; km ²)	675	1344	1117	117	644	540	1403	841	1326	2947	477	4977
Alluvial groundwater area (AGA; km ²)	29	178	76	11	37	24	70	108	33	82	56	30
Non-alluvial groundwater area (NAGA; km ²)	39	98	206	0	507	406	1104	729	840	1903	10	3908
AGA * 100/TCA (%)	4	13	7	9	6	4	5	13	2	3	12	1
NAGA * 100/TCA (%)	6	7	18	0	79	75	79	87	63	65	2	79
Polluted alluvial groundwater ^a (km ²)	16	98	17	11	0	22	0	46	2	0	56	0
Polluted alluvial groundwater ^a (% of the AGA)	54	55	23	97	0	91	0	42	5	0	100	0
Polluted non-alluvial groundwater ^a (km ²)	0	0	0	0	0	0	33	0	0	0	0	0
Polluted non-alluvial groundwater ^a (% of the NAGA)	0	0	0	0	0	0	3	0	0	0	0	0
Estimated NVZ ^b (km ²)	89	263	65	10	29	21	256	272	254	494	63	638
NVZ officially designated (km ²)	0	93	7	0	0	0	0	150	0	82	21	0
Altitude (m) ^c												
Min.	545	428	408	386	360	342	264	494	289	275	311	299
Mean	944	895	1068	642	1192	977	859	632	648	631	567	896
Max.	2029	2269	2211	1418	2164	1763	1708	1372	1384	1491	1166	2881
Precipitation (mm yr ⁻¹) ^d												
Min.	525	481	440	477	467	450	360	739	412	406	446	417
Mean	650	628	666	488	642	555	476	892	733	966	571	932
Max.	806	819	815	541	757	682	622	1209	1058	1527	719	1491

^a [NO₃⁻] ≥ 50 mg L⁻¹.

^b Our proposal of NVZ extracted from Model A (Fig. 7).

^c Altitude above sea level (extracted from a DEM of 10 m resolution).

^d Extracted from Botey et al. (2013).

Table 2

Land use class	Crop Type ^a	N-surplus (kg N ha ⁻¹ yr ⁻¹)	Irrigated land (%)	Irrigation system (%)		
				Furrow	Sprinkler	Drip
Horticultural crops	Vegetables (all brassicas, leafy or stalked vegetables, vegetables cultivated for fruit, pulses, cultivated mushrooms and other vegetables)	154 ± 5 ^a	88 ^b	15 ^b	30 ^b	55 ^b
	Root crops (potatoes, sugar beet, and other tubers)	171 ± 5 ^a	76 ^b	14 ^b	79 ^b	7 ^b
	Flower crops	184 ± 11 ^a	88 ^b	15 ^b	30 ^b	55 ^b
Herbaceous forage crops	Herbaceous forage crops	69 ± 9 ^a	25 ^b	55 ^b	45 ^b	0 ^b
Other herbaceous crops	Cereals (wheat, barley, rye, oat, grain maize, sorghum, triticale, other cereals)	25 ± 14 ^a	16 ^b	50 ^b	48 ^b	2 ^b
	Dried pulses	13 ± 4 ^a	6 ^b	18 ^b	81 ^b	1 ^b
	Industrial crops (oilseeds, textile crops, tobacco and other industrial crops)	3 ± 13 ^a	21 ^b	25 ^b	55 ^b	20 ^b
Citrus crops	Citrus fruit crops	170 ± 13 ^a	93 ^b	19 ^b	0 ^b	81 ^b
Fruit tree crops	Fruit tree crops (excluding citrus)	72 ± 12 ^a	28 ^b	19 ^b	2 ^b	79 ^b
Other woody crops	Almond trees	24 ± 4 ^a	0 ^b	0 ^b	0 ^b	0 ^b
	Vineyards	17 ± 6 ^a	38 ^b	2 ^b	3 ^b	95 ^b
	Olive trees	7 ± 20 ^a	28 ^b	6 ^b	0 ^b	94 ^b
	Other trees	10 ± 3 ^a	4 ^b	11 ^b	10 ^b	79 ^b
Meadows and pastures	Grazing areas	11 ± 1 ^a	8 ^d			
Forest areas	-	1 ^c	-			

^a Source: MAGRAMA (2013, 2015a) and MAPAMA (2016, 2017).
^b Source: MAGRAMA (2015b).
^c Estimated from Forest Europe (2015).
^d Source: SIOSE (2011).

from fertilisers, manure, livestock and stubble burning (European Commission, 2018). As leaching losses are not considered in these estimations, net N-balance surpluses give information on the availability of nitrogen to be dispersed via leaching, according to each crop type. Data on net N-balances in agricultural crops are to be annually reported by member countries to the European Union.

A semi-quantitative risk assessment of N-losses to groundwater, associated with agricultural land use, was developed using information on the annual net N-balance surpluses in Spanish crops from 2011 to 2015 (Table 2). Data were extracted from annual reports on the net N-balance in Spanish agriculture (MAGRAMA, 2013, 2015a; MAPAMA, 2016, 2017). The corresponding information for Spanish forests was extracted from Forest Europe (2015).

To better visualize the relative risk scale, the annual averages of N-surplus in Spanish crops for the period 2011–2015 were ln-transformed and ordered, by crop type, from highest to lowest value to meet linearity (Fig. 2). To confirm the linear relationship between

an ordinal qualitative variable (crop type) and a quantitative variable (ln of N-surplus) a simple linear regression was performed. Thereafter, ratings (for the risks of N-leaching associated with land use) were assigned to the dependent variable on a scale from 1 to 10, and classified into five risk categories (according to Arauzo, 2017) as follows: negligible risk: 1–2; low risk: 3–4; moderate risk: 5–6; high risk: 7–8; extreme risk: 9–10.

With regard to irrigation efficiency, Waskom et al. (1994) estimated water-use efficiencies of about 90%, 75% and 40% for drip, sprinkler and conventional furrow irrigation methods, respectively. As low-efficient irrigation systems contribute to N-leaching, the dominant irrigation system for each crop type was considered as part of the risk assessment. For that, the coverages of irrigated land and types of irrigation system in Spanish crops were extracted from MAGRAMA (2015b); Table 2). For typical rainfed crops but managed under irrigation, overloads were applied to the initially estimated ratings (Fig. 2) with the following criteria: for crops with

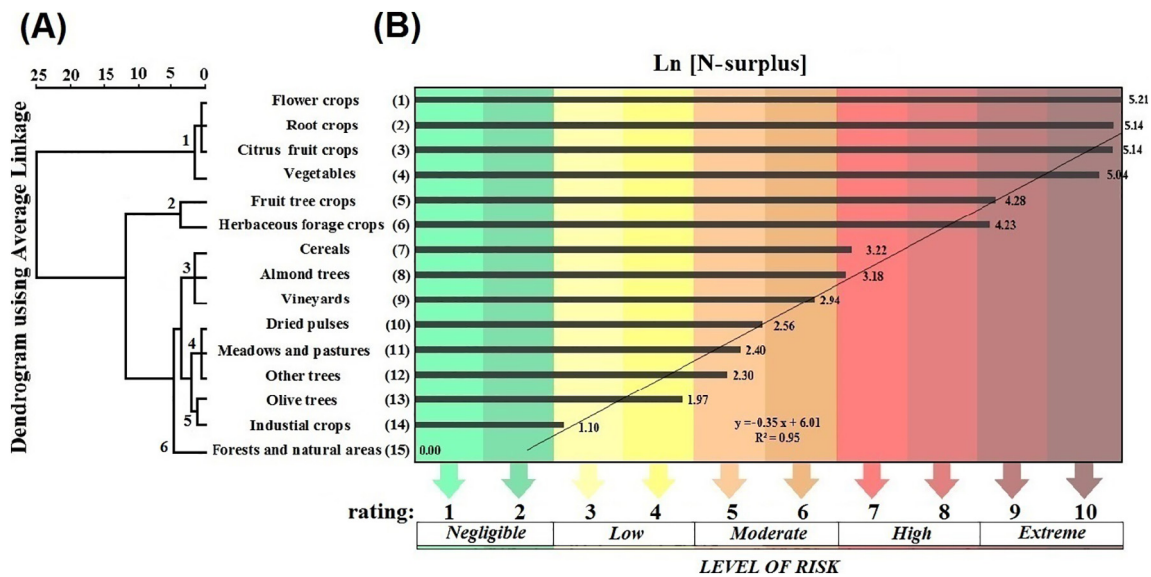


Fig. 2. Risk assessment of N-loss to groundwater associated with land use: (A) Dendrogram resulting from the hierarchical cluster analysis of the annual N-surpluses in Spanish crops from 2011 to 2015; main groups are numbered from 1 to 6; (B) Crop types (ordered from highest to lowest potential risk) vs. mean annual N-surpluses in Spanish crops from 2011 to 2015 (ln-transformed to meet linearity); ratings assigned to risks of N-leaching were classified into five risk categories according to Arauzo (2017).

irrigated land coverages below 30% and >60% watered by conventional furrow or sprinkler irrigation (Table 2), an overload of +1 was added to the initial ratings (Fig. 2) to compensate for the low irrigation efficiency; for the same crops managed under rainfed conditions (coverages above 70%), no overload was applied.

Regarding non-agricultural sources of N-loss, the ratings assigned to land use categories such as fish and livestock farms (point pollution sources), urban areas (point and multipoint sources) and unproductive land (nonpoint sources), were based on Secunda et al. (1998), Buschmann (2001) and Lerner (2000). These land uses were scarcely represented in the study area compared to the large extensions of agricultural and natural areas (MARM, 2009; SIOSE, 2011).

3.2. Catchment areas

All thematic maps in this study were prepared using the software ArcGIS 10.3 for Desktop (ESRI, Redlands, CA, USA; ESRI, 2015) and the coordinate reference system ETRS89/UTM zone 30N. The catchment areas of the 12 alluvial aquifers were delineated from a digital elevation model (DEM) of 10 m resolution, using the Hydrology toolset in the Spatial Analyst Toolbox (ArcGIS 10.3). The lowest elevation point for each alluvial aquifer was used as pour point for watershed calculation. The pour point was defined as the cell of highest flow accumulation, at which water flows out of an area (outlet location from the flow accumulation).

3.3. Nitrate mapping

The map of nitrate concentration in groundwater was generated from the average nitrate concentrations from 2011 to 2015 at 290 monitoring points (irrigation wells, boreholes and springs). Hydrochemical data were provided by the Ebro Hydrographic Confederation (Confederación Hidrográfica del Ebro, 2019). Groundwater samples were collected, mostly on a seasonal basis. To create the map for the study area, the Spline Interpolation tool in the Spatial Analyst Toolbox (ArcGIS 10.3) was applied, aquifer by aquifer, to the shapefiles of points representing the average nitrate concentrations in groundwater.

3.4. The LU-IV procedure

The LU-IV procedure (Arauzo, 2017; Fig. 3) was devised for mapping groundwater vulnerability to nitrate pollution, with the final goal of improving the NVZ delineation. The method is notable for: (1) using simple and readily available parameters to feed the model, (2) avoiding assigning insufficiently contrasted weights to the parameters, and (3) assessing the entire catchment area that potentially drains into a receptor aquifer.

The procedure is a two-step GIS-based method that combines a map of intrinsic vulnerability (based on the IV index; Arauzo, 2017) with a map of the risks of N-leaching associated with land use. The model assigns ratings on a scale from 1 to 10, for both maps of intrinsic vulnerability (Step 1) and specific vulnerability to nitrate pollution

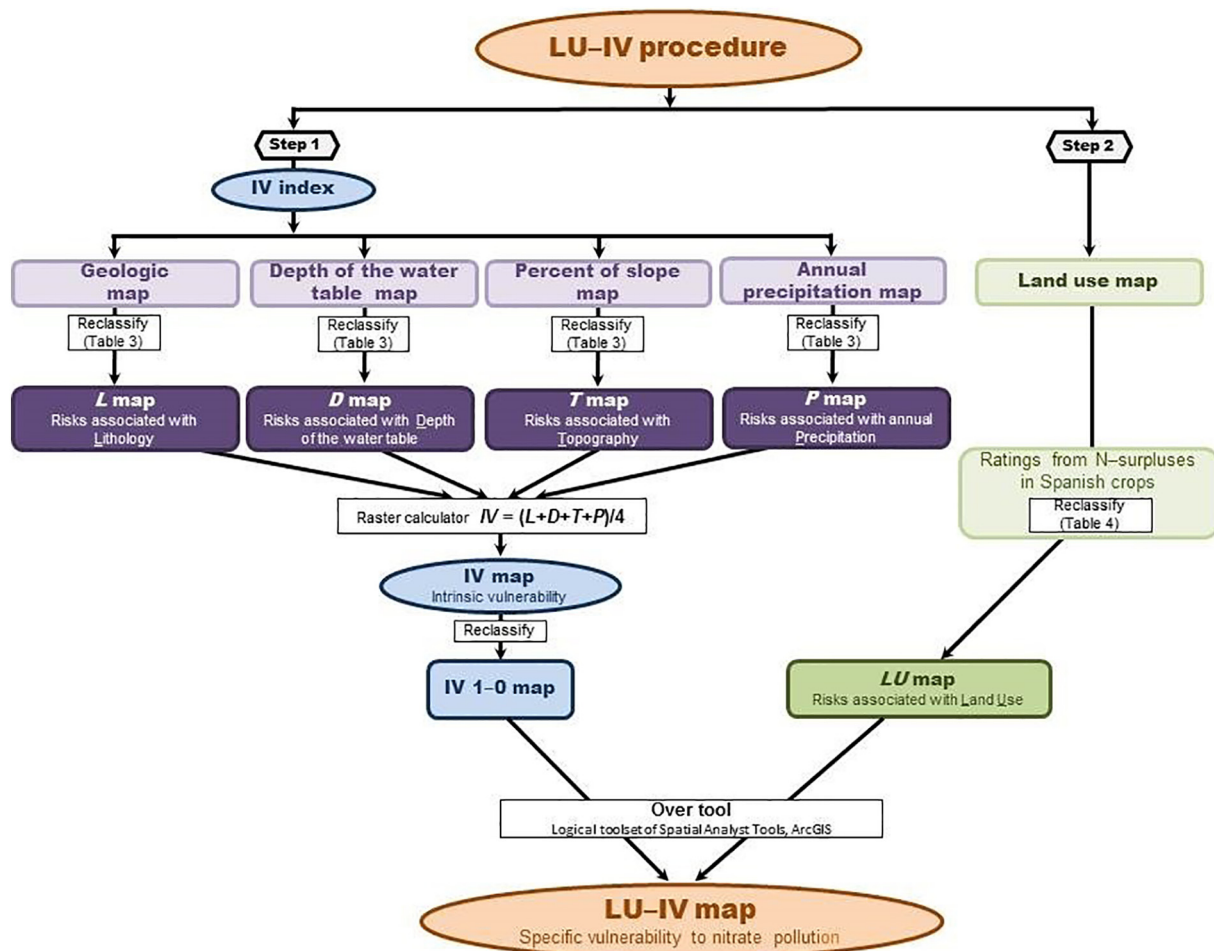


Fig. 3. The LU-IV procedure.

(Step 2). Ratings are classified into five risk categories: negligible: 1–2; low: 3–4; moderate: 5–6; high: 7–8; extreme: 9–10.

In Step 1, the IV index is used to map the intrinsic groundwater vulnerability. In its most basic formulation, the index uses four environmental parameters as follows:

$$IV = \frac{L + D + T + P}{4} \quad (1)$$

where L is the rating of the risks associated with the lithology of the vadose zone, D is the rating of the risks associated with the depth of the water table, T is the rating of the risks associated with topography (percentage of slope), and P is the rating of the risks associated with average annual precipitation.

Ratings for the parameters that make up the IV index are shown in Table 3. A more detailed description of the index IV can be found in Arauzo (2017).

The map of intrinsic vulnerability based on the IV index was generated from the raster maps of parameters L , D , T and P , using the Raster Calculator in the Spatial Analyst Toolbox (ArcGIS 10.3) to run the Eq. (1). The raster maps of L , D and P were generated using data from IGME (2015; *Geologic digital map of Spain at a scale of 1:50,000*), Confederación Hidrográfica del Ebro (data provided in Excel format

and Botey et al. (2013), respectively. The map of T was generated from a DEM of 10 m resolution, using the Slope tool in the Spatial Analyst Toolbox (ArcGIS 10.3).

In Step 2, the map of intrinsic vulnerability (from the IV index) and a map of the risks of N-leaching associated with land use are combined, using the Over tool from the Math>Logical toolset of Spatial Analyst Tools (ArcGIS 10.3). For this, we must first reclassify the original cell values of the raster of intrinsic vulnerability into values of “1” and “0”. The value “1” represents non-vulnerable areas (cell values ranging from 1 to 4: negligible to low vulnerability) and the value “0” represents vulnerable areas (cell values ranging from 5 to 10: moderate to extreme vulnerability). The resulting raster (intrinsic vulnerability 1–0) is then used as the first entry in the Over tool, while the raster of risks associated with land use (LU map) is used as the second entry. When the Over operation is performed, for cell values in the first input that are equal to “1” the output value will be that of the first input (representing areas in which land use restrictions do not have to be applied). But where the cell values in the first input correspond to “0”, the output will be that of the second input raster (original ratings of the raster of risks associated with land use). Through this procedure, we obtain a map of groundwater vulnerability to nitrate pollution associated with land use, from which we can draw polygons delimiting the NVZ by using the Conversion Tools (ArcGIS 10.3). Additional information on the design and applicability of the LU–IV procedure can be found in Arauzo (2017).

Finally, to complete the second entry of the Over tool we need a raster map of the risks of N-loss associated with land use (previously referred to as LU map). To generate an accurate LU map a good land use base map is required (preferably at a scale of at least 1:50,000) as well as a fine-tuned risk rating system that represents the different risks associated with land use (results from the 1st objective). In this paper, two different maps of land use of Spain (MARM, 2009, and SIOSE, 2011) were tested for use as the base map to generate the LU map (described in the next section). Once the Over tool was applied, the maps of specific vulnerability resulting from the LU–IV procedure (using the new ratings of the risks associated with land use) were compared with the following maps of groundwater vulnerability based on previous models for assessing groundwater vulnerability: first version of the LU–IV procure (which uses LU ratings from bibliographical references; extracted from Arauzo, 2017), DRASTIC model (extracted from IGME, 2009a, 2009b) and GOD model (extracted from Arauzo, 2014).

3.5. Testing two base maps to generate the map of risks associated with land use

There are two maps of land use of Spain that potentially could be used as base maps for generating the raster map of risks associated with land use: (1) the Map of Crops and Land Use of Spain 2000–09 (Mapa de Cultivos y Aprovechamientos de España 2000–09 – Spanish–; MARM, 2009; hereinafter referred as MCAE 2000–09), and (2) the Map of Land Cover and Use Information System of Spain, SIOSE 2011 (Mapa del Sistema de Información sobre Ocupación del Suelo de España SIOSE 2011 –Spanish–; SIOSE, 2011; IGN, 2015; hereinafter referred as SIOSE, 2011). Their pros and cons as base maps and other characteristics are indicated below.

MCAE 2000–09 was produced during the period 2000–09, at a scale of 1:50,000. It is the update of an earlier version from 1980 to 1990. In this cartography, crops and land use are delimited by polygons of single coverage and described by codes of land use and overloads. Originally, the digital version of MCAE 2000–09 used the coordinate reference system ED50/UTM zone 30N, which was reprojected to ETRS89/UTM zone 30N for this project. The shapefiles of MCAE 2000–09 were provided by the Spanish Ministry of the Environment and Rural and Marine Affairs. Shapefiles were clipped and merged to cover the study area. Then, the attribute table was completed by assigning the new LU ratings (Table 4) to the polygons. The resultant shapefile LU map (using

Table 3
Ratings for the environmental parameters that make up the IV index.

Lithology of the vadose zone (L) ^a	Rating	Depth to the water table (D) ^b (m)	Rating
Calcretes, karst limestones; gravels	10	0–1 (and all depths for calcretes, karst limestones, chalky limestones, calcarenites, recent volcanic lavas and gravels)	10
Chalky limestones, calcarenites	9	>1–3	9
Alluvial and fluvio–glacial sands; recent volcanic lavas	7–8	>3–5	8
Aeolian sands; volcanic tuffs; igneous/metamorphic formations and older volcanic formations; sandstones, conglomerates; peat	5–6	>5–10	7
Alluvial silts, loess, glacial till, loam; mudstones; shales	3–4	>10–13	6
Clays; residual soils	1–2	>13–20 >20–33 >33–50 >50 No underlying aquifer	5 4 3 2 1
Annual precipitation (P) (mm yr ^{−1})	Rating	Topography (T) ^c (% of slope)	Rating
>900	10	0–2	10
>800–900	9	>2–3	9
>700–800	8	>3–4	8
>600–700	7	>4–5	7
>500–600	6	>5–6	6
>400–500	5	>6–9	5
>300–400	4	>9–12	4
>200–300	3	>12–15	3
>100–200	2	>15–18	2
0–100	1	>18	1

^a Based on lithological character and degree of consolidation (Foster et al., 2002) and hydraulic conductivity and permeability (Bear, 1972).

^b Adapted from Foster et al. (2002).

^c According to Aller et al. (1987).

MCAE 2000–09 and *LU* ratings from N-surpluses in Spanish crops) was extracted into a raster format, to be used as the second entry of the Over tool of the LU–IV procedure.

SIOSE 2011 satisfies current Spanish National and Regional Administration requirements on Land Cover and Use information (IGN, 2015). SIOSE's objective was to generate a soil occupancy database for all of Spain, at a scale of 1:25,000. Its coordinate reference system is ETRS89/UTM zone 30N. SIOSE divides the territory according to a continuous mesh of polygons, where each polygon is assigned a type of coverage (polygons of single coverage) or a combination of them (polygons of composite coverage, mosaic or association). Different surface minimum units are used according to the cover class in the land (urban fabric and water bodies: 1 ha; agricultural land, forest and natural areas: 2 ha; wetlands, beaches, greenhouses, riverside vegetation: 0.5 ha). SIOSE has been produced since 2005, with updates in 2009 and 2011. The shapefiles of SIOSE 2011 were provided by the Spanish National Geographic Institute (SIOSE, 2011). Shapefiles were clipped and merged to cover the study area. Then, the attribute table was completed by assigning the new *LU* ratings (Table 4) to the polygons; in polygons of single coverage (homogeneous areas with a single land use), the same

rating was applied to the entire polygon; in polygons of composite coverage, mosaic or association (areas with a mix of land uses, divided in subpolygons), the assigned rating was calculated as the weighted arithmetic mean of the ratings for the different land uses in the subpolygons (proportionally to their respective areas). The resultant shapefile *LU* map (using SIOSE 2011 and *LU* ratings from N-surpluses in Spanish crops) was then extracted into a raster format, to be used as second entry of the Over tool of the LU–IV procedure.

3.6. Statistical analysis

A hierarchical cluster analysis using between-group linkage and Euclidean distance measure (IBM SPSS Statistics 25.0; IBM Corp. Released, 2017) was performed to identify groups of crops with similar annual N-surpluses (as part of the risk assessment of N-losses associated with land use). For this, the annual net N-surpluses in different Spanish crops from 2011 to 2015 (MAGRAMA, 2013, 2015a; MAPAMA, 2016, 2017) were used.

The Band Collection Statistics tool in the Spatial Analyst Toolbox (ArcGIS 10.3) was used to generate a Pearson correlation matrix to compare, on a regional scale, the rasters of: (1) nitrate concentration in groundwater, (2) vulnerability to nitrate pollution using the LU–IV procedure based on MCAE 2000–09 and using *LU* ratings from N-surpluses (model A), (3) vulnerability to nitrate pollution using the LU–IV procedure based on SIOSE 2011 and *LU* ratings from N-surpluses (model B), (4) vulnerability to nitrate pollution using the LU–IV procedure based on MCAE 2000–09 and *LU* ratings from bibliographical references (extracted from Arauzo, 2107; model C), (5) the IV index (model D), (6) the DRASTIC index (model E), and (7) the GOD index (model F). Previously, the rasters were clipped to have the same geographic extent as that of the smallest extent (map of nitrate concentration in groundwater). This statistical approach, however, was not sensitive to the spatial discordances that can occur between nitrate vulnerable areas (at the land surface) and groundwater polluted areas (in the saturated zone). Such common discrepancies are a consequence of the long-distance advective transport of nitrate from the highest to the lowest areas of catchments (Zahid et al., 2015) and accumulation/dilution processes within the saturated zone (Arauzo and Martínez-Bastida, 2015).

To overcome the above-mentioned limitation, a statistical approach that considered processes at catchment scale was applied. Within a catchment, a direct proportionality could be expected between the estimated area of NVZ and the area of groundwater affected by nitrate pollution. On this basis, one-tailed Pearson and Spearman correlation coefficient analyses were conducted to test which models of vulnerability could be the best predictors of nitrate pollution (IBM SPSS Statistics 25.0), applied to the alluvial aquifers (the most affected groundwater bodies), as well as to the totality of groundwater bodies within each catchment. Correlations were performed between the area (or the relative area) of NVZ at high-extreme risk (estimated from the models A to F) and the area of groundwater that was already polluted or/and at risk of being polluted by nitrate, in each of the 12 alluvial catchments ($n = 12$). The relative areas of NVZ, expressed as a percentage of the total catchment area, were used for correlations with the areas of alluvial aquifers affected by nitrate (given their small size with respect to the wide variability in the size of their catchment areas). Before, the Kolmogorov–Smirnov normal distribution test was applied to determine whether a parametric correlation test (r) or a non-parametric test (ρ) should be employed to analyse the data (IBM SPSS Statistics 25.0).

4. Results and discussion

4.1. Risk assessment of N-losses associated with land use

Balanced fertilization, so as to limit total nitrogen input with fertiliser to crop requirements, has been scarcely implemented in the

Table 4

Ratings for the risks associated with land use. Risk assessment was based on the annual N-surpluses in Spanish crops (Fig. 2).

Land use/crop type	Water use: rainfed or irrigated ^a	<i>LU</i> rating
Horticultural crops (vegetables, root crops and flower crops)	Generally irrigated (84%): mainly sprinkler and drip irrigation	10
Citrus crops	Generally irrigated (93%): mainly drip irrigation	10
(Irrigated) Herbaceous forage crops	If irrigation (25%): mainly furrow and sprinkler irrigation (+1)	10 ^b
Herbaceous forage crops	Generally rainfed (75%)	9
Fruit tree crops	Generally rainfed (72%). If irrigation (28%): mainly drip irrigation	9
(Irrigated) Cereals	If irrigation (16%): mainly furrow and sprinkler irrigation (+1)	8 ^b
Cereals	Generally rainfed (84%)	7
Fish farms	–	5–8 (7) ^c
Livestock farms	–	5–8 (7) ^c
Urban areas	–	5–8 (7) ^c
Almond trees	Rainfed (100%)	7
Vineyards	Generally rainfed (62%). If irrigation (38%): drip irrigation	6
(Irrigated) Dried pulses	If irrigation (6%): mainly sprinkler and furrow irrigation (+1)	6 ^b
(Irrigated) Meadows	If irrigation (8%): mainly sprinkler and furrow irrigation (+1)	6 ^b
Dried pulses	Generally rainfed (94%)	5
Meadows and pastures	Generally rainfed (92%)	5
Other trees	Generally rainfed (96%). If irrigation (4%): mainly drip irrigation	5
Olive trees	Generally rainfed (72%). If irrigation (28%): mainly drip irrigation	4
(Irrigated) Industrial crops	If irrigation (21%): mainly sprinkler and furrow irrigation (+1)	4 ^b
Industrial crops	Generally rainfed (79%)	3
Shrubland	–	1–5 (3) ^d
Unproductive land	–	1–5 (2) ^c
Forests and natural areas	–	1

^a Coverages of rainfed and irrigated land in Spanish crops are shown (as percentage of the total area of the crop type; MAPAMA, 2015b).

^b An overload of +1 was applied when low-efficient irrigation systems were dominant (conventional furrow and sprinkler irrigation; Table 2).

^c Sources: Secunda et al. (1998), Buschmann (2001) and Lerner (2000); preferred rating between brackets.

^d Source: Arauzo (2017); preferred rating between brackets.

EU so far, resulting in large amounts of N-surplus on agricultural land (Environment Agency, 2017). In view of this, the net N-balance surplus in Spanish crops was used as a predictive indicator of the potential impact of the different types of crops on groundwater quality.

The dendrogram from the cluster analysis of the annual N-surpluses (from 2011 to 2015) revealed a hierarchy of pressures and potential impacts depending on the amount of N-surplus, allowing six main groups of crop type to be defined (Fig. 2A). Groups, ordered from highest to lowest risk of N-loss, were as follows: (1) horticultural and citrus fruit crops, (2) other fruit tree crops and herbaceous forage crops, (3) cereals, almond trees and vineyards, (4) dry pulses, meadows and pastures, other trees, (5) olive trees and industrial crops and (6) forest and natural areas. N-surplus ranged from 170 kg N ha⁻¹ yr⁻¹ in group 1, 69–72 kg N ha⁻¹ yr⁻¹ in group 2, 17–25 kg N ha⁻¹ yr⁻¹ in group 3, 11–15 kg N ha⁻¹ yr⁻¹ in group 4, 3–7 kg N ha⁻¹ yr⁻¹ in group 5 and 1 kg N ha⁻¹ yr⁻¹ in group 6 (Table 2). Interannual variability was low, especially in the high risk groups.

Linearity between crop types, ordered from highest to lowest potential risk (ordinal qualitative independent variable), and annual N-surplus (ln-transformed quantitative dependent variable) was used to generate a risk rating scale (Fig. 2B). Groups of crop types (Fig. 2A) were then classified into five preliminary risk categories: extreme

(groups 1 and 2), high (group 3), moderate (groups 3 and 4), low (group 5) and negligible (group 6). This semi-quantitative approach was further refined by adding overloads to those crops irrigated with low-efficiency technologies (MAGRAMA, 2015b; Table 2). The resultant ratings (Table 4) represented the potential risks of N-leaching from different Spanish crops according to their annual N-balance and irrigation efficiency. These new ratings differ to those proposed by Secunda et al. (1998), as follows: (1) horticultural crops (new rating: 10; Secunda et al.: 8); (2) citrus crops (new rating: 10; Secunda et al.: 7); (3) irrigated/rainfed herbaceous forage crops (new ratings: 10–9; Secunda et al.: 8–4); (4) fruit tree crops (new rating: 9; Secunda et al.: 6); (5) rainfed cereals (new rating: 7; Secunda et al.: 4); (6) dry pulses (new rating: 5; Secunda et al.: 4); and (6) irrigated/rainfed industrial crops (new ratings: 4–3; Secunda et al.: 10–4). Note that some ratings increased from high to extreme risk, and from low to moderate/high/extreme risk. Results confirmed the suggestion of Sutton et al. (2011) that irrigated agriculture is the major contributor to nitrate pollution in groundwater, and the findings of Arauzo and Valladolid (2013) who reported significant N-losses to groundwater from rainfed herbaceous crops associated with precipitation.

The ratings in Table 4 are required to generate the map of the risks associated with land use (LU map), which in turn is used to complete

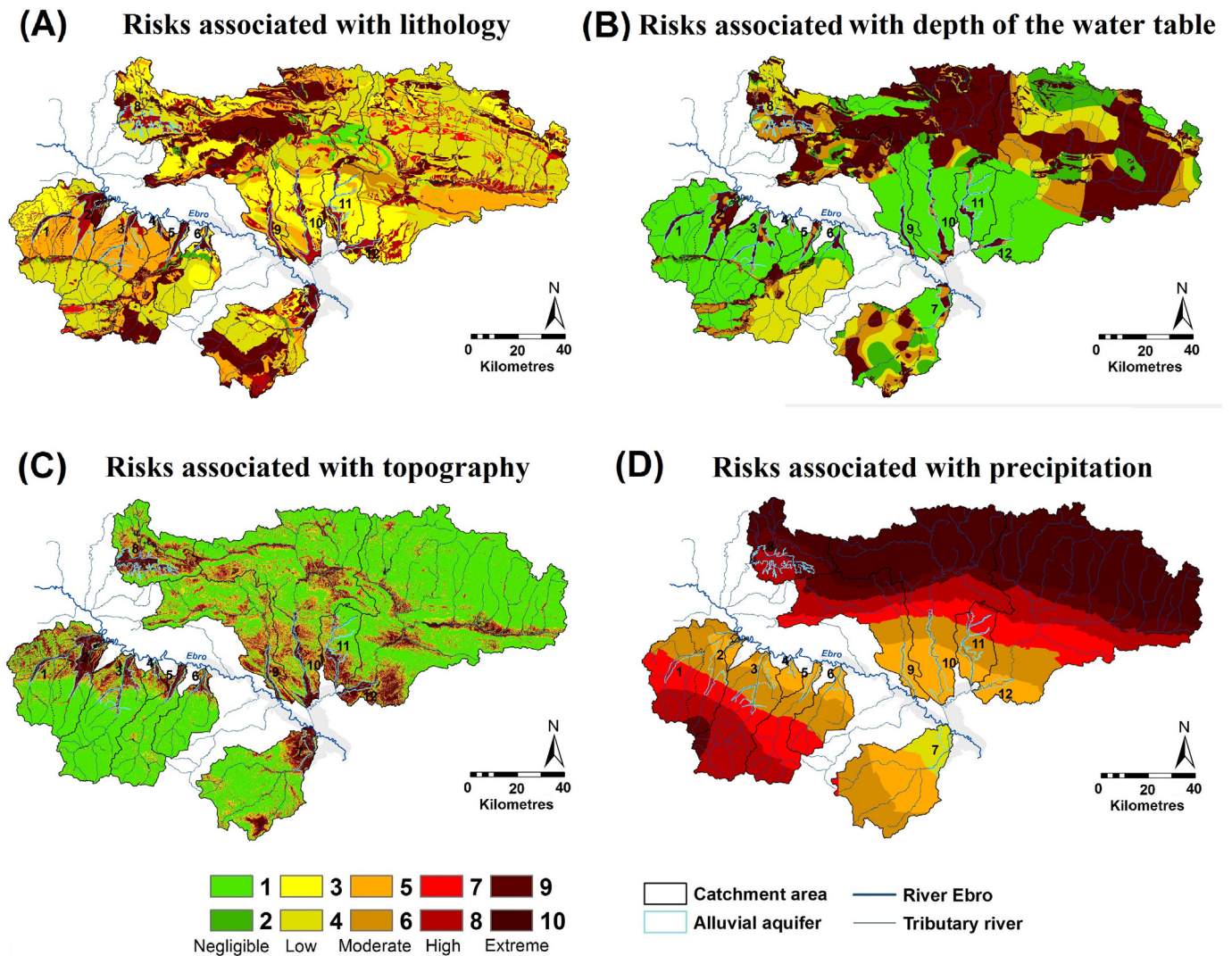


Fig. 4. Thematic maps that make up the IV index: (A) map of the risks associated with the lithology of the vadose zone; (B) map of the risks associated with the depth of the water table; (C) map of the risks associated with topography (percentage of slope); (D) map of the risks associated with the annual precipitation.

the map of groundwater vulnerability to nitrate pollution according to the LU-IV procedure.

4.2. Nitrate pollution

Groundwaters with nitrate concentrations that exceed 50 mg L^{-1} are considered polluted, while those between 25 and 50 mg L^{-1} are considered at risk of pollution (European Commission, 2000). According to these guidelines, 67% of the alluvial aquifers of the study area contained polluted areas, 25% had areas at risk and only 8% remained free of nitrate pollution (Fig. 1). Of the polluted alluvial aquifers, 42% were affected in more than one-half of their surface (aquifers of rivers Tirón, Oja, Río Antiguo, Alhama and Cidacos; Table 1). It was also observed that nitrate tended to accumulate at the lower, flatter sections of the alluvial areas, defined as stagnant zones by Arauzo (2017).

Nitrate pollution in non-alluvial groundwater bodies was, however, barely represented. Only one aquifer (comprised of conglomerates, sandstones and sandy limestone) was polluted in 3% of its area in catchment no. 7 (Table 1 and Fig. 1). Catchments 9, 10 and 12 showed areas at risk (Fig. 1) in carbonate-rock and sandstone aquifers.

Nitrate concentration in groundwater can be reduced by mixing (diluting water with a high nitrate concentration with water of a lower concentration) and by attenuation (with denitrification as the most significant mass removal process) (Rivett et al., 2008). However, the contribution of other catchment parameters to nitrate dynamics at catchment scale is still to be explored. In relation to the role of catchment size in the 12 alluvial catchments under analysis (Table 1), we found significant positive correlations between catchment area and maximum altitude ($r = 0.60, p \leq 0.05$) and mean and maximum precipitation ($r = 0.70, p \leq 0.05$ and $r = 0.81, p \leq 0.01$, respectively). This suggests that the largest catchments, which in these cases present mountain headwater systems (as the Pyrenees, Basque mountains and Iberian System) associated with high precipitations, are able to provide

greater water availability and, therefore, a greater dilution capacity. The negative correlation between catchment area and polluted alluvial area (expressed as % of the AGA, Table 1; $r = -0.60, p \leq 0.05$) confirmed that the greater the extension of the catchment (the higher dilution capacity), the lower the incidence of nitrate pollution in the alluvial area.

4.3. IV index

The IV index allowed assessment of the intrinsic vulnerability in the entire topographic surface (12 alluvial catchments) that potentially drains nitrate-polluted waters into the alluvial aquifers (Fig. 1). The four thematic maps that make up the IV index (Fig. 4) represent different aspects of vulnerability associated with lithological, hydrological, topographic and climatic attributes. According to lithology and degree of water table exposure, alluvial deposits and limestones were the most vulnerable substrates (Fig. 4A, B). Alluvial deposits also presented a high risk associated with topography, since most of their surfaces generally occupy the flatter, lower areas of the catchments, where nitrate tend to accumulate (Arauzo, 2017). However, the risk associated with precipitation in alluvial areas was mostly moderate, precisely because of their lower altitudes (Fig. 4C, D). In contrast, limestone substrates presented a lower risk associated with topography (because they are generally located in mountain areas, which implies high slopes) but a higher risk associated with precipitation (Fig. 4C, D).

The map of intrinsic vulnerability (Fig. 5) shows that: (1) all alluvial areas were in a high-extreme risk category, which coincided with the high levels of nitrate contents in alluvial groundwater in most of the catchments (no. 1, 2, 3, 4, 6, 8, 9 and 11; Fig. 1); (2) catchments that drain from the Pyrenees and Basque mountains (no. 8, 9, 10 and 12) were intrinsically vulnerable in >50% of their surfaces (Table 1; Figs. 1 and 4); (3) carbonate aquifer systems (in catchments no. 8, 9, 10 and 12) had large areas with high-extreme intrinsic vulnerability that did not coincide with high nitrate levels in the groundwater (Fig. 1); and

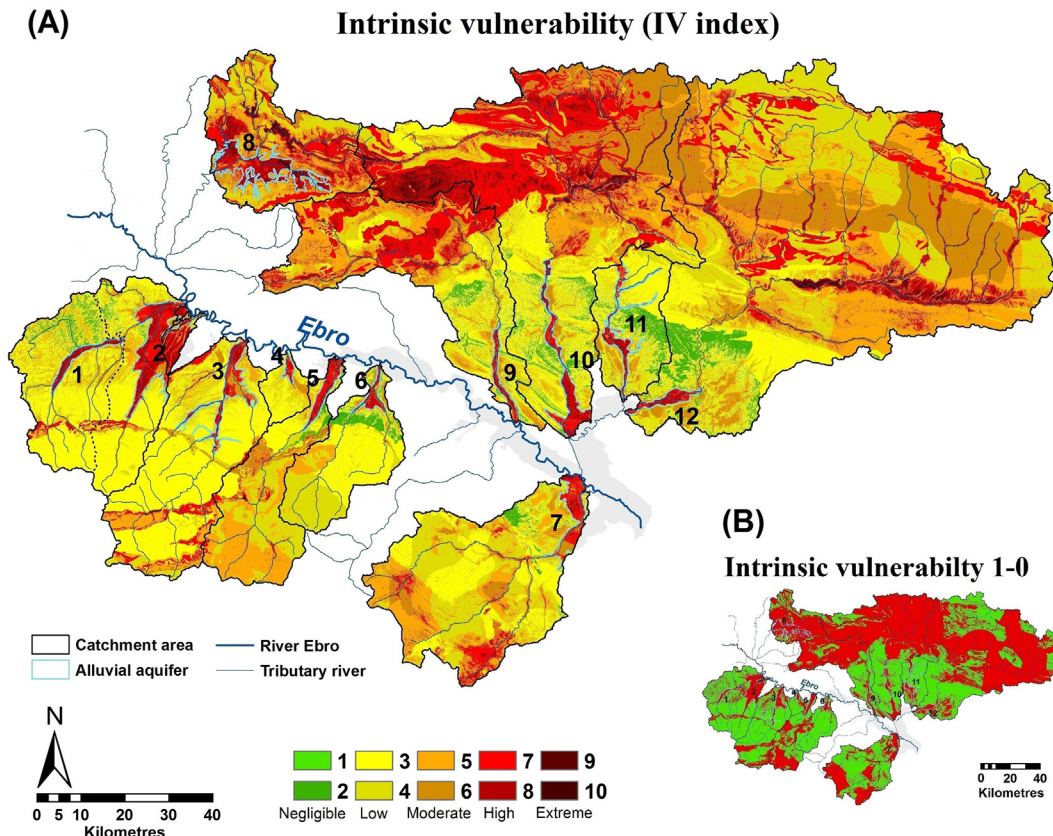


Fig. 5. (A) Map of the intrinsic vulnerability (IV index); (B) Map of the intrinsic vulnerability 1-0.

(4) in the areas without underlying groundwater (Fig. 1) intrinsic vulnerability ranged from negligible to moderate.

Discrepancy between the high-extreme intrinsic vulnerability in the carbonate aquifers in the northern part of the study area and the absence of high levels of nitrate content in groundwater can be explained by two non-exclusive factors: (1) according to Arauzo (2017), it is expected that forests and natural areas in mountain headwaters are protecting land uses that do not generate contamination (despite the high intrinsic vulnerability); and (2) limited information on the degree of karstification of carbonate rocks might have eventually led to an over-estimation of the ratings assigned to parameters *L* and *D* (Table 3).

4.4. LU-IV procedure: versions based on MCAE 2000–09 and SIOSE 2011

A new approach to the LU-IV procedure was proposed by applying the new *LU* ratings based on the *N*-surpluses. For this, the map of intrinsic vulnerability (Fig. 5) was combined with a map of the risks associated with land use (*LU* map; Fig. 6) to obtain the map of specific vulnerability to nitrate pollution.

To generate the *LU* map, the *LU* ratings resulting from the analysis of *N*-surpluses in Spanish crops (Table 4) were applied to a base map of land use. In this part of the investigation, two different land use cover maps of Spain were tested as base maps: the Map of Crops and Land Use of Spain 2000–09 (MCAE 2000–09) and the Map of Land Cover and Use Information System of Spain (SIOSE, 2011). The two resulting versions of the *LU* map looked reasonably similar (Fig. 6A, B), albeit with differences of nuance. In both, high-extreme risk zones (mostly comprised of horticultural crops, herbaceous forage crops and cereals) were distributed towards the middle and/or lower areas of the catchments. The exceptions were catchments no. 7, 8 and 11, in which the risks extended over a large part of the catchment.

When comparing MCAE 2000–09 and SIOSE 2011 as base maps, there are several aspects that should be considered, such as: mapping scale, frequency of updates, how information is organized and represented, and the usefulness of the information. MCAE 2000–09 is at a scale of 1:50,000, while SIOSE 2011 is at 1:25,000. MCAE 2000–09 is the second update of a previous version from 1980 to 90. SIOSE has been produced since 2005, with updates in 2009 and 2011, so its update rate may favour revisions of designated NVZ (mandatory for EU members every four years). Regarding the process of assigning the *LU* ratings

(Table 4), land uses in MCAE 2000–09 are delimited by polygons of single coverage (described by land use and overload codes). In SIOSE 2011, there are polygons of single coverage and polygons of composite coverage, mosaic or association, which make the assignment of ratings much more difficult. Furthermore, SIOSE 2011 does not allow distinction between the coverages of different herbaceous crops (horticultural crops, herbaceous forage crops and cereals) that are included under the same descriptor code (although attribute descriptors partially compensate for this). MCAE 2000–09 does not allow distinction between irrigated herbaceous forage crops and irrigated cereals (which is not a major limitation because most of these crops are usually managed under rainfed conditions; Table 2). Finally, SIOSE 2011 provides detailed information on artificial coverages, while MCAE 2000–09 does not offer this information. In view of the pros and cons, we did not find definitive reasons to choose, *a priori*, between MCAE 2000–09 and SIOSE 2011 as base map, so we will have to wait for validation and comparison of the different models of vulnerability.

The land use maps from MCAE 2000–09 and SIOSE 2011 (Fig. 6A, B) were used to generate the respective versions of the map of vulnerability to nitrate pollution using the LU-IV procedure (Fig. 7A, B), with reasonably close results.

Subsequently, potential NVZ were extracted from the different models of vulnerability (Fig. 8) and compared with the map of nitrate content in groundwater, both at regional and catchment scale. The models analysed were the following: model A (LU-IV procedure, based on MCAE 2000–09 and using land use ratings from *N*-surpluses in Spanish crops), model B (LU-IV procedure, based on SIOSE 2011 and using land use ratings from *N*-surpluses in Spanish crops), model C (LU-IV procedure, based on MCAE 2000–09 and using land use ratings from bibliographical references; Arauzo, 2017), model D (IV index), model E (DRASTIC index) and model F (GOD index).

As a preliminary validation (at regional scale), we generated a correlation matrix of the raster of nitrate concentration in groundwater and the rasters of groundwater vulnerability based on models A–F (Table 5). This statistical approach revealed significant positive relationships between the seven variables, which was not surprising due to the high number of degrees of freedom ($n-2 = 16,640,795$), but the results allowed verification that models A, B and C (of specific vulnerability based on the LU-IV procedure) had much better correlations with nitrate concentration in groundwater than models D, E and F (of intrinsic

(A) Risks associated with land use using MCAE 2000-09 as base map
Based on the annual *N*-surpluses in Spanish crops

(B) Risks associated with land use using SIOSE 2011 as base map
Based on the annual *N*-surpluses in Spanish crops

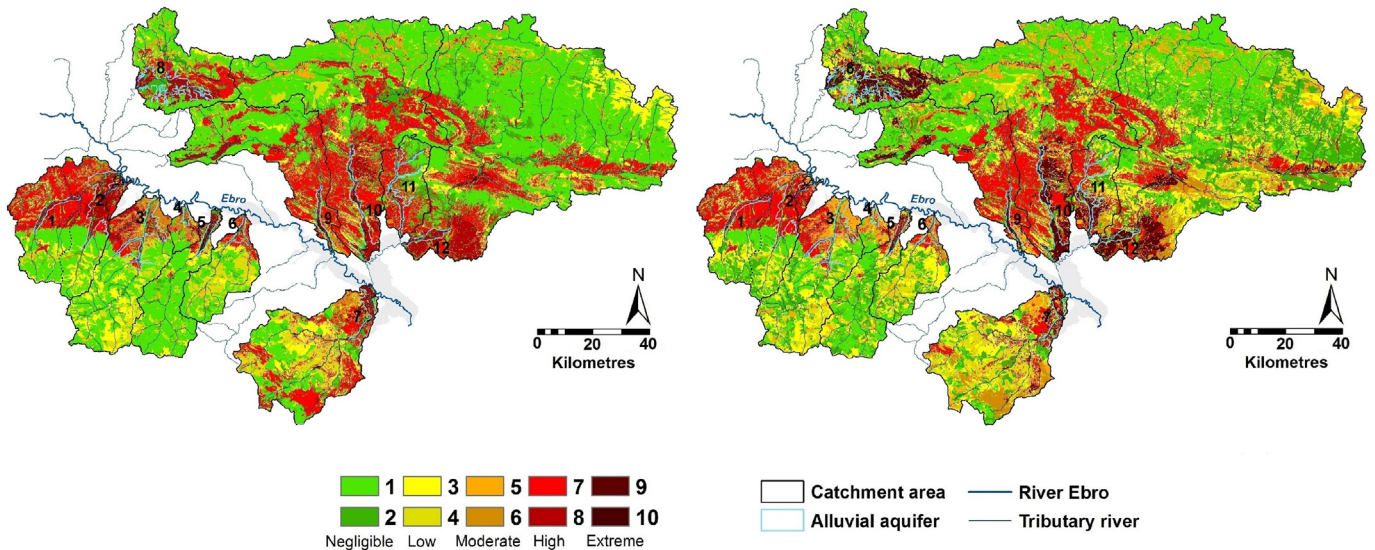


Fig. 6. Two versions of the map of the risks associated with land use (*LU* map): (A) using MCAE 2000–09 as base map; (B) using SIOSE 2011 as base map. *LU* ratings applied to both base maps were estimated from the annual *N*-balance surpluses in Spanish crops (Table 4).

vulnerability). However, as explained above, a correlation matrix of rasters cannot be considered a method that is sensitive to the spatial discrepancies between nitrate vulnerable areas (at the land surface) and areas of polluted groundwater (in the saturated zone), which are explained by advective transport of nitrate and accumulation/dilution

processes within the vadose and the saturated zones (Arauzo and Martínez-Bastida, 2015).

To address the above-mentioned limitation, additional validations were performed that took into account the processes occurring at catchment scale. For this, correlations between the area of NVZ (from models

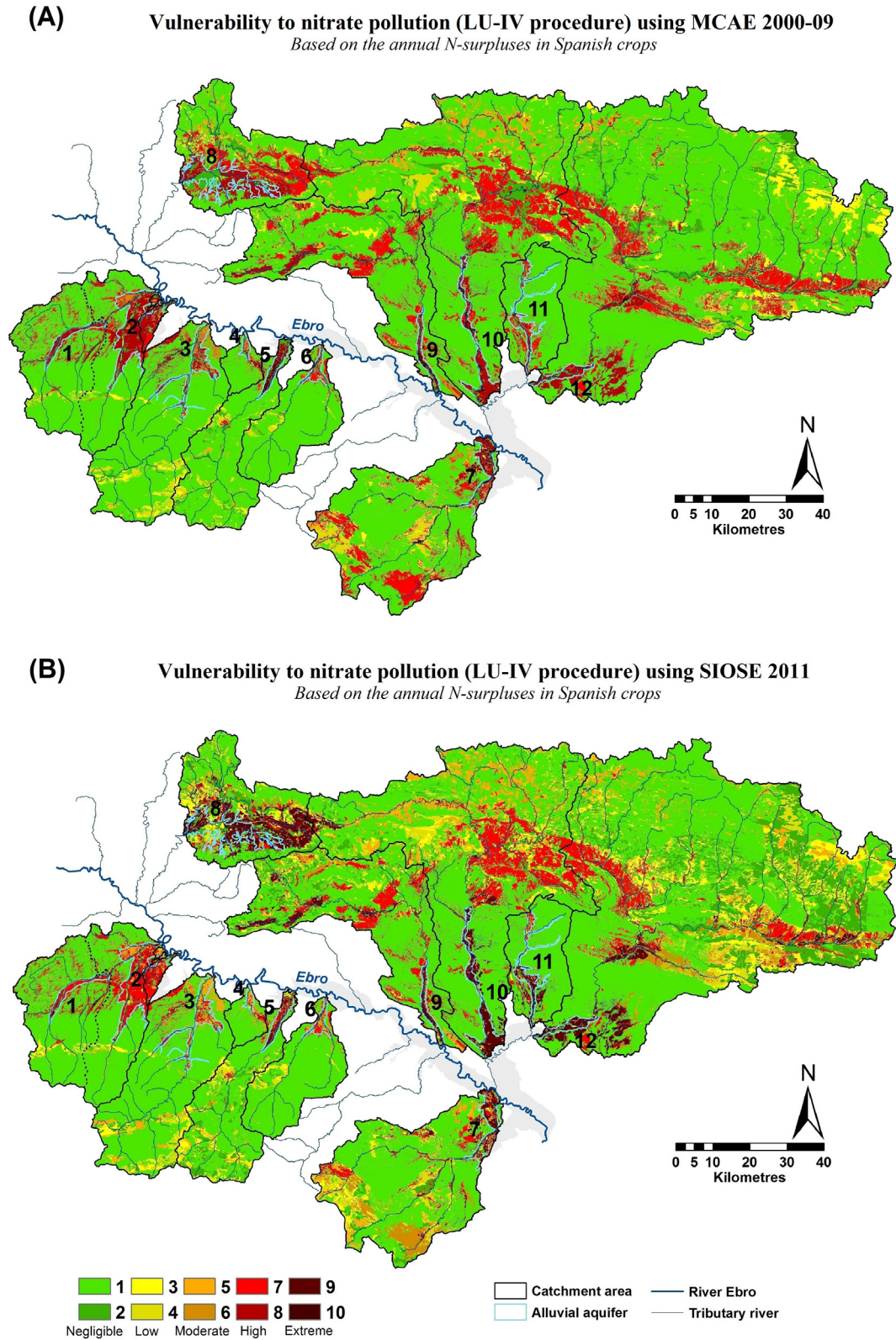


Fig. 7. Two versions of the map of vulnerability to nitrate pollution (LU-IV procedure): (A) using MCAE 2000-09 for the LU map (Fig. 6A); (B) using SIOSE 2011 for the LU map (Fig. 6B).

Table 5
Correlation matrix of the rasters of nitrate concentration in groundwater and different models of groundwater vulnerability (labelled from A to F) to compare the parameters to each other at regional scale; $n = 16,640,797$ (number of pixels); due to large degrees of freedom all correlations were statistically significant with at least $p \leq 0.001$.

	[NO ₃ ⁻]	MODEL (A): LU-IV based on MCAE (NEW)	MODEL (B): LU-IV based on SIOSE (NEW)	MODEL (C): LU-IV based on MCAE (Arauzo, 2017)	MODEL (D): IV index	MODEL (E): DRASTIC index	MODEL (F): GOD index
[NO ₃ ⁻]	1.00						
MODEL (A): LU-IV procedure based on MCAE 2000–09; LU ratings from N-surpluses in Spanish crops (NEW)	0.34	1.00					
MODEL (B): LU-IV procedure based on SIOSE, 2011; LU ratings from N-surpluses in Spanish crops (NEW)	0.31	0.88	1.00				
MODEL (C): LU-IV procedure based on MCAE 2000–09; LU ratings from bibliographical references (Arauzo, 2017)	0.33	0.83	0.81	1.00			
MODEL (D): IV index	0.13	0.38	0.43	0.40	1.00		
MODEL (E): DRASTIC index (extracted from IGME, 2009a,b)	0.12	0.25	0.26	0.28	0.38	1.00	
MODEL (F): GOD index (extracted from Arauzo, 2014)	0.12	0.16	0.18	0.22	0.66	0.34	1.00

A to F) and the area of groundwater (including alluvial and non-alluvial aquifers) that was already polluted or at risk of being polluted by nitrate (above 25 mg L⁻¹), estimated for each of the 12 catchments (Table 6), were analysed. The results confirmed the expectations, with remarkable higher significance for models A and B (which used the LU-IV procedure with the new LU ratings from N-surpluses in Spanish crops).

Another validation was performed using only the information on alluvial aquifers (the most affected by nitrate pollution). Correlations between the relative area of NVZ (from models A to F) and the areas of alluvial groundwater with over 25 mg L⁻¹ of nitrate (including zones that were polluted and at risk of being polluted) and over 50 mg L⁻¹ (only polluted zones) showed similar results (Table 7). Again, models A and B proved to be the best predictors, both for polluted alluvial areas and for areas at risk. Taken together, these results confirm the high level of reliability of the LU-IV procedure, when LU ratings obtained empirically from N-surplus crops are applied.

Models A and B (which used MCAE 2000–09 and SIOSE 2011 as base maps, respectively) offered fairly similar results, although model A gave a slightly better fit to the validation data. According to model A, the 12 catchments can be ordered from highest to lowest relative extent of NVZ (representing high to extreme levels of vulnerability) as follows: catchment no. 8 (32%; 272 km²) > no. 2 (20%; 263 km²) > no. 9 (19%; 254 km²) > no. 7 (18%; 256 km²) > no. 10 (17%; 494 km²) > no. 12 (13%; 638 km²) = no. 1 (13%; 89 km²) = no. 11 (13%; 63 km²) > no. 4 (8%; 10 km²) > no. 3 (6%; 65 km²) > no. 5 (5%; 29 km²) > no. 6 (4%, 31 km²) (Table 1; Fig. 8). Considering the totality of the catchments, the estimated NVZ covered a surface of 2454 km² (15% of the study area). These results contrast with the 354 km² officially designated as NVZ (2% of the study area).

5. Conclusions

The net N-balance surplus in Spanish crops has proved to be a useful predictive indicator of the risks of N-loss to groundwater from agricultural nonpoint sources. A hierarchical cluster analysis of the annual amounts of N-surplus in Spanish crops revealed six distinct clusters, ordered from highest to lowest potential risk of N-loss as follows: (1) horticultural and citrus fruit crops, (2) other fruit tree crops and herbaceous forage crops, (3) cereals, almond trees and vineyards, (4) dry pulses, meadows and pastures, other trees, (5) olive trees and industrial crops, and (6) forest and natural areas.

Annual data on net N-surpluses were used to generate a detailed risk rating system reflecting the potential risks of N-loss associated with land use. The rating system was fine-tuned with information on irrigation efficiency in Spanish crops. The new empirical LU ratings (Table 4) were used to assess the specific vulnerability of groundwater to nitrate pollution in a GIS environment, by using the LU-IV procedure (Arauzo, 2017; a GIS-based method that combines a map of intrinsic vulnerability with a map of the risks of N-loss associated with land use).

Environmental variability among the catchment areas of 12 alluvial aquifers (associated with tributaries of the Ebro River basin, Spain) provided the necessary conditions to assess and validate the new approach to the LU-IV procedure. Eight of these 12 alluvial aquifers showed nitrate concentrations exceeding 50 mg L⁻¹, while the others presented areas at risk or were free of pollution. Nitrate pollution in the non-alluvial groundwater bodies of the study area was barely represented.

The role of the catchment size was revealed as a key factor in the emergence of groundwater areas affected by nitrate pollution. It was shown that the largest catchments (having mountain headwater systems associated with high precipitations) are able to provide greater

Table 6
One-tailed Pearson (r) and Spearman correlations (ρ) between the area of NVZ at high-extreme risk (estimated from models A to F; Fig. 7) and the area of groundwater^a that was already polluted or at risk of being polluted by nitrate (above 25 mg L⁻¹) in each of the 12 catchments under study ($n = 12$). The Kolmogorov–Smirnov normal distribution test was applied to determine whether a parametric or a non-parametric test should be employed.

Area of NVZ (km ²)	vs.	Area of groundwater ^a polluted or at risk ([NO ₃ ⁻] ≥ 25 mg L ⁻¹ ; km ²)	
MODEL (A): LU-IV procedure based on MCAE 2000–09; LU ratings from N-surpluses in Spanish crops (NEW)		$r = 0.91$	$P\text{-value} = 0.00002$
MODEL (B): LU-IV procedure based on SIOSE, 2011; LU ratings from N-surpluses in Spanish crops (NEW)		$r = 0.82$	$P\text{-value} = 0.0005$
MODEL (C): LU-IV procedure based on MCAE 2000–09; LU ratings from bibliographical references (Arauzo, 2017)		$r = 0.70$	$P\text{-value} = 0.01$
MODEL (D): IV index		$r = 0.70$	$P\text{-value} = 0.01$
MODEL (E): DRASTIC index (extracted from IGME, 2009a, b)		$\rho = 0.60$	$P\text{-value} = 0.02$
MODEL (F): GOD index (extracted from Arauzo, 2014)		$\rho = 0.45$	$P\text{-value} = 0.07$

^a Including alluvial and non-alluvial groundwater bodies.

Table 7

One-tailed Pearson (r) and Spearman correlations (ρ) between the relative area of NVZ at high–extreme risk (estimated from models A to F; Fig. 7) and the areas of alluvial groundwater with over 25 mg L^{-1} of nitrate (including zones that were polluted and at risk of being polluted) and over 50 mg L^{-1} (only polluted zones) in each of the 12 alluvial catchments ($n = 12$). The relative areas of NVZ were expressed as a percentage of the total catchment area (% of the TCA). The Kolmogorov–Smirnov normal distribution test was applied to determine whether a parametric or a non-parametric test should be employed.

Relative area of NVZ (% of the TCA)	vs.	Area of alluvial groundwater (km^2)			
		Polluted or at risk [NO ₃ ⁻] $\geq 25 \text{ mg L}^{-1}$		Polluted [NO ₃ ⁻] $\geq 50 \text{ mg L}^{-1}$	
MODEL (A): LU–IV procedure based on MCAE 2000–09; LU ratings from N–surpluses in Spanish crops (NEW)		$r = 0.63$	$P\text{-value} = 0.01$	$r = 0.47$	$P\text{-value} = 0.06$
MODEL (B): LU–IV procedure based on SIOSE, 2011; LU ratings from N–surpluses in Spanish crops (NEW)		$r = 0.69$	$P\text{-value} = 0.01$	$r = 0.46$	$P\text{-value} = 0.06$
MODEL (C): LU–IV procedure based on MCAE 2000–09; LU ratings from bibliographical references (Arauzo, 2017)		$r = 0.52$	$P\text{-value} = 0.04$	$r = 0.38$	$P\text{-value} = 0.11$
MODEL (D): IV index		$r = 0.48$	$P\text{-value} = 0.05$	$r = 0.01$	$P\text{-value} = 0.40$
MODEL (E): DRASTIC index (extracted from IGME, 2009a,b)		$\rho = 0.18$	$P\text{-value} = 0.29$	$\rho = -0.28$	$P\text{-value} = 0.18$
MODEL (F): GOD index (extracted from Arauzo, 2014)		$\rho = 0.43$	$P\text{-value} = 0.08$	$\rho = 0.34$	$P\text{-value} = 0.14$

water availability and, therefore, a greater dilution capacity of the dissolved pollutants.

The map of intrinsic vulnerability (IV index) showed that all the alluvial aquifers were at a high–extreme risk level, coinciding with the high nitrate levels in alluvial groundwater in most of the catchments. Carbonate aquifer systems also showed large areas of high–extreme intrinsic vulnerability which, however, did not coincide with high nitrate concentrations in the groundwater. This discrepancy can be explained by two non-exclusive factors: (1) forests and natural areas in mountain headwaters are protecting land uses that do not generate contamination, despite the high intrinsic vulnerability; and (2) limited information on the degree of karstification of carbonate rocks might have eventually led to overestimation of the ratings assigned to parameters *L* and *D*.

The maps of *LU* from two different base maps (MCAE 2000–09 and SIOSE 2011) were used to generate the respective versions of the map of vulnerability to nitrate pollution using the LU–IV procedure, with reasonably close results. Subsequently, potential NVZ were extracted from different models of vulnerability and compared with the map of nitrate content in groundwater. The models compared were the following: model A (LU–IV procedure, based on MCAE 2000–09 and using *LU* ratings from N–surpluses in Spanish crops), model B (LU–IV procedure, based on SIOSE 2011 and using *LU* ratings from N–surpluses in Spanish crops), model C (LU–IV procedure, based on MCAE 2000–09 and using *LU* ratings from bibliographical references; Arauzo, 2017), model D (IV index), model E (DRASTIC index) and model F (GOD index). After three different validations (at regional and catchment scales) the results confirmed, as expected, that models A and B (which used the LU–IV procedure with the new *LU* ratings from N–surpluses) proved to be the best predictors, both for at risk and polluted groundwater areas. These results support the high level of reliability of the LU–IV procedure when applying the *LU* ratings obtained empirically from the N–surpluses. Our best estimation of NVZ (based on Model A) covered a surface area of 2454 km^2 (15% of the study area). These results differ considerably from the 354 km^2 officially designated as NVZ (2% of the study area).

The proposed risk rating system, based on N–surpluses in Spanish crops which represent the potential risks of N–loss to groundwater from agricultural diffuse sources, could be exportable to other countries of the Mediterranean area of similar climatic and agricultural conditions to those of Spain.

Acknowledgements

The authors acknowledge the Spanish State Research Agency and the European Regional Development Fund for their financial support of Project CGL2016–81110–R (AEI/FEDER, UE). We thank the Ebro Hydrographic Confederation for providing the hydrochemical data and

the digital version of the geologic map of the River Ebro basin. The digital map of Land Cover and Use Information System of Spain SIOSE 2011 was provided by the Spanish National Geographic Institute. The digital map of Crops and Land Use in Spain 2000–09 was provided by the Spanish the Ministry of the Environment and Rural and Marine Affairs.

References

- Aller, L., Bennet, T., Lehr, J.H., Petty, R.J., 1987. DRASTIC. A Standardized System for Evaluating Groundwater Pollution Potential Using Hydrogeologic Settings (U.S. EPA Report 600/2–87–035, Oklahoma).
- Arauzo, M., 2014. Groundwater vulnerability to nitrate pollution in the upper River Ebro basin: GOD index and risks associated with land use (Vulnerabilidad de las aguas subterráneas a la contaminación por nitrato en la Cuenca Alta del Ebro: índice GOD y riesgos asociados a los usos del territorio; Spanish). In: Gómez-Hernández, J.J., Rodrigo-Ilari, J. (Eds.), *II Congreso Ibérico de las Aguas Subterráneas: CIAS 2014 Valencia*. Editorial Universitat Politècnica de València, Valencia, pp. 33–54.
- Arauzo, M., 2017. Vulnerability of groundwater resources to nitrate pollution: a simple and effective procedure for delimiting nitrate vulnerable zones. *Sci. Total Environ.* 575, 799–812. <https://doi.org/10.1016/j.scitotenv.2016.09.139>.
- Arauzo, M., Martínez-Bastida, J.J., 2015. Environmental factors affecting diffuse nitrate pollution in the major aquifers of central Spain: groundwater vulnerability vs. groundwater pollution. *Environ. Earth Sci.* 73, 8272–8286. <https://doi.org/10.1007/s12665-014-3989-8>.
- Arauzo, M., Valladolid, M., 2013. Drainage and N–leaching in alluvial soils under agricultural land uses: implications for the implementation of the EU nitrates directive. *Agric. Ecosyst. Environ.* 179, 94–107. <https://doi.org/10.1016/j.agee.2013.07.013>.
- Arqued, V.M., 2018. It is likely that the areas designated as nitrate vulnerable zones will be expanded (Es probable que se amplíen las zonas declaradas como vulnerables por la contaminación con nitratos agrícolas, Spanish). *Tierras Agric.* 268, 120–122.
- Bear, J., 1972. *Dynamic of Fluids in Porous Media*. Dover Publications, Inc, New York.
- Botey, R., Guijarro, J.A., Jiménez, A., 2013. Normal Monthly Precipitation from 1981–2010 (Valores Normales de precipitación Mensual 1981–2010; Spanish). Dirección de Producción e Infraestructuras, Agencia Estatal de Meteorología (AEMET), Ministerio de Agricultura, Alimentación y Medio Ambiente, Madrid.
- Buschmann, A.H., 2001. Environmental Impact of Aquaculture; the State of Research in Chile and the World. A Bibliographic Analysis of Advances and Restrictions for a Sustainable Production in Aquatic Systems (Impacto Ambiental de la Acuicultura; el Estado de la investigación en Chile Y el Mundo. Un análisis bibliográfico de los Avances Y Restricciones Para Una producción Sustentable en los Sistemas acuáticos; Spanish). Terram Publicaciones, Santiago de Chile.
- Commission of the European Communities, 2007. Report from the Commission to the Council and the European Parliament on Implementation of Council Directive 91/676/EEC Concerning the Protection of Waters against Pollution Caused by Nitrates from Agricultural Sources for the Period 2000–2003 (SEC (2007) 339). / COM/2007/0120 Final*, Brussels.
- Confederación Hidrográfica del Ebro, 2018. SITEbro. Geodata. <http://iber.chebro.es/geoportal/>, Accessed date: 3 September 2018.
- Confederación Hidrográfica del Ebro, 2019. State and quality of water. Groundwater. Quality. Analytical data query (Estado y calidad de las aguas. Aguas subterráneas. Calidad. Consulta de datos analíticos; Spanish). <http://www.datossubterranas.chebro.es:81/WCAS/>, Accessed date: 4 January 2019.
- Council of the European Communities, 1991. Council Directive 91/676/EEC of 12 December 1991 concerning the Protection of Waters against Pollution caused by Nitrates from Agricultural Sources. Off. J. Eur. Union L 375. Annex I, Brussels.
- De Clercq, P., Gertsis, A.C., Hofman, G., Jarvis, S.C., Neeteson, J.J., Sinabell, F. (Eds.), 2001. *Nutrient Management Legislation in European Countries*. Ghent University, Department of Soil Management and Soil Care, Ghent.
- Economic and Social Council of the United Nations, 2018. Special Edition: Progress towards the Sustainable Development Goals. Report of the Secretary-General. Chapter II: Where we Are in the Achievement of the Sustainable Development.

- Goal 6, Ensure Availability and Sustainable Management of Water and Sanitation for all. <https://undocs.org/E/2019/68>, Accessed date: 29 July 2019.
- ESRI, 2015. ArcGIS Desktop: Release 10.3. Environmental Systems Research Institute, Redlands, CA.
- European Commission, 2000. Nitrates Directive (91/676/EEC). Status and Trends of Aquatic Environment and Agricultural Practice. Development Guide for Member States' Reports. Directorate-General for Environment, Brussels.
- European Commission, 2018. Commission Staff Working Document Accompanying the Document Report From the Commission to the Council and the European Parliament on the Implementation of Council Directive 91/676/EEC Concerning the Protection of Waters against Pollution Caused by Nitrates From Agricultural Sources Based on Member State Reports for the Period 2012–2015 (COM (2018) 257 Final), Brussels.
- European Environment Agency, 2017. Agricultural Land: Nitrogen Balance. Environmental Indicator Report 2017 – In Support to the Monitoring of the 7th Environment Action Programme. EEA Report No 21/2017, Brussels.
- Forest Europe, 2015. State of Europe's Forests 2015. Ministerial Conference on Protection of Forests in Europe. FOREST EUROPE, Madrid.
- Foster, S.S.D., 1987. Fundamental concepts in aquifer vulnerability, pollution risk and protection strategy. In: van Duijvenbooden, W., van Waegeningh, H.G. (Eds.), Vulnerability of Soil and Groundwater to Pollution, Proceedings and Information No. 38. TNO Committee on Hydrological Research, the Netherlands, pp. 69–86.
- Foster, S.S.D., Hirata, R., Gómez, D., D'Elia, M., Paris, M., 2002. Ground Water Quality Protection. A Guide for Water Utilities, Municipal Authorities and Environment Agencies. The World Bank, Washington D.C.
- IBM Corp. Released, 2017. IBM SPSS Statistics for Windows, Version 25.0. IBM Corp, Armonk, NY.
- IGME, 2009a. Map of Groundwater Vulnerability to Pollution. Reduced Version of the DRASTIC Index. Ebro River Basin. Assessment of the Intrinsic Vulnerability of Intercommunity Groundwater. Detritic and Mixed Masses (Mapa de Vulnerabilidad a la contaminación del Agua subterránea. Índice DRASTIC Reducido. Demarcación Hidrográfica del Ebro. Evaluación de la Vulnerabilidad intrínseca de Las Aguas subterráneas Intercomunitarias. Masas detríticas y Mixtas; Spanish) [Map in Digital Format]. 1:1,000,000. Instituto Geológico y Minero de España, Dirección General del Agua <http://www.igme.es/>, Accessed date: 5 September 2017.
- IGME, 2009b. Map of Groundwater Vulnerability to Pollution. Reduced Version of the DRASTIC Index. Ebro River Basin. Assessment of the Intrinsic Vulnerability of Intercommunity Groundwater. Carbonated Masses (Mapa de Vulnerabilidad a la Contaminación del Agua subterránea. Índice DRASTIC Reducido. Demarcación Hidrográfica del Ebro. Evaluación de la Vulnerabilidad intrínseca de las Aguas subterráneas Intercomunitarias. Masas carbonatadas; Spanish) [Map in Digital Format]. 1:1,000,000. Instituto Geológico y Minero de España, Dirección General del Agua <http://www.igme.es/>, Accessed date: 5 September 2017.
- IGME, 2015. Geological map of Spain, MAGNA series; Geological and Mining Institute of Spain (Mapa geológico de España, series MAGNA; Instituto Geológico y Minero de España; Spanish) [maps in digital format]. 1:50,000. <http://iber.chebro.es/geoportal/>, Accessed date: 10 December 2015.
- IGN, 2015. Land Cover and Use Information System of Spain. SIOSE 2011 Technical Paper. Version 1.1 (Sistema de Información de Ocupación del Suelo en España. Documento Técnico SIOSE 2011. Versión 1.1; Spanish). Instituto Geográfico Nacional, Ministerio de Fomento, Madrid.
- Kumar, P., Bansod, B.K.S., Debnath, S.K., Kumar Thakur, P., Ghanshyam, C., 2015. Index-based groundwater vulnerability mapping models using hydrogeological settings: a critical evaluation. Environ. Impact Assess. Rev. 51, 38–49. <https://doi.org/10.1016/j.ear.2015.02.001>.
- Lerner, D., 2000. Guidelines for Estimating Urban Loads of Nitrogen to Groundwater. Defra Project Report, NT1845, Sheffield.
- Machiwal, D., Jha, M.K., Singh, V.P., Mohan, C., 2018. Assessment and mapping of groundwater vulnerability to pollution: current status and challenges. Earth-Sci. Rev. 185, 901–927. <https://doi.org/10.1016/j.earscirev.2018.08.009>.
- MAGRAMA, 2013. Nitrogen balance in Spanish agriculture for the year 2011 (Balance del nitrógeno en la agricultura española, año 2011; Spanish). Ministerio de Agricultura y Pesca, Alimentación y Medio Ambiente, Secretaría General Agricultura y Alimentación, Dirección General de Producciones y Mercados Agrarios, Madrid.
- MAGRAMA, 2015a. Nitrogen balance in Spanish agriculture for the year 2013 (Balance del nitrógeno en la agricultura española, año 2013; Spanish). Ministerio de Agricultura y Pesca, Alimentación y Medio Ambiente, Secretaría General Agricultura y Alimentación, Dirección General de Producciones y Mercados Agrarios, Madrid.
- MAGRAMA, 2015b. Survey on crop areas and yields. Report on irrigation in Spain (Encuesta sobre superficies y rendimientos de cultivos. Informe sobre regadíos en España; Spanish). Ministerio de Agricultura y Pesca, Alimentación y Medio Ambiente, Secretaría General Técnica, Subdirección General de Estadística, Madrid.
- MAPAMA, 2016. Nitrogen Balance in Spanish Agriculture for the Year 2014 (Balance del nitrógeno en la agricultura española, año 2014; Spanish). Ministerio de Agricultura y Pesca, Alimentación y Medio Ambiente, Secretaría General Agricultura y Alimentación, Dirección General de Producciones y Mercados Agrarios, Madrid.
- MAPAMA, 2017. Nitrogen Balance in Spanish Agriculture for the Year 2015 (Balance del nitrógeno en la agricultura española, año 2014; Spanish). Ministerio de Agricultura y Pesca, Alimentación y Medio Ambiente, Secretaría General Agricultura y Alimentación, Dirección General de Producciones y Mercados Agrarios, Madrid.
- MARM, 2009. Map of Crops and Land Use in Spain 2000–09 (Mapa de Cultivos y Aprovechamientos de España 2000–09; Spanish) [Maps in Digital Format]. 1: 50,000. Ministerio de Medio Ambiente, Medio Rural y Marino de España, Madrid.
- Martínez-Bastida, J.J., Arauzo, M., Valladolid, M., 2010. Intrinsic and specific vulnerability of groundwater in central Spain: the risk of nitrate pollution. Hydrogeol. J. 18, 681–698. <https://doi.org/10.1007/s10040-009-0549-5>.
- Pisciotta, A., Cusimano, G., Favara, R., 2015. Groundwater nitrate risk assessment using intrinsic vulnerability methods: a comparative study of environmental impact by intensive farming in the Mediterranean region of Sicily, Italy. J. Geochem. Explor. 156, 89–100. <https://doi.org/10.1016/j.gexplo.2015.05.002>.
- Rivett, M.O., Buss, S.R., Morgan, P., Smith, J.W.N., Bemment, C.C., 2008. Nitrate attenuation in groundwater: a review of biogeochemical controlling processes. Water Res. 42, 4215–4232. <https://doi.org/10.1016/j.watres.2008.07.020>.
- Secunda, S., Collin, M.L., Melloul, A.J., 1998. Groundwater vulnerability assessment using a composite model combining DRASTIC with extensive agricultural land use in Israel's Sharon region. J. Environ. Manag. 54, 39–57. <https://doi.org/10.1006/jema.1998.0221>.
- SIOSE, 2011. SIOSE 2011 Land Cover and Use Information System of Spain (SIOSE 2011 Sistema de Información sobre Ocupación del Suelo de España; Spanish) [Maps in Digital Format]. 1:25,000. ©Instituto Geográfico Nacional, Madrid <http://centrodedescargas.cnig.es/CentroDescargas/busquedaSerie.do?codSerie=SIOSE>, Accessed date: 5 April 2017.
- Sutton, M.A., Howard, C.M., Erisman, J.W., Billen, G., Bleeker, A., Grennfelt, P., van Grisen, H., Grizzetti, B., 2011. The European Nitrogen Assessment: Sources, Effects and Policy Perspectives. Cambridge University Press, Cambridge.
- Waskom, R.M., Cardon, G.E., Crookston, M.A., 1994. Best Management Practices for Irrigation Agriculture. A Guide for Colorado Producers. Colorado Water Resources Research Institute, Colorado State University, Fort Collins, Colorado Grant No.14–08–0001–G2008/3, Project No. 2, Completion Report No. 184.
- Worrall, F., Spencer, E., Burt, T.P., 2009. The effectiveness of nitrate vulnerable zones for limiting surface water nitrate concentrations. J. Hydrol. 370, 21–28. <https://doi.org/10.1016/j.jhydrol.2009.02.036>.
- Zahid, A., Hassan, M.Q., Ahmed, K.M.U., 2015. Simulation of flowpaths and travel time of groundwater through arsenic-contaminated zone in the multi-layered aquifer system of Bengal Basin. Environ. Earth Sci. 73, 979–991. <https://doi.org/10.1007/s12665-014-3447-7>.